

Three Long Lived Excited States of Tm^-

Steven M. O'Malley and Donald R. Beck

Physics Department, Michigan Technological University, Houghton, MI

(Dated: July 20, 2004)

Considering p , d , and f attachments to the $4f^{13}6s^2$ $J = 7/2$ ground state of Tm I, we find no evidence for bound Tm^- states. A survey of possible weak attachments to excited Tm I states, however, suggests three long lived states created by $6p$ attachment to the $4f^{12}5d6s^2$ $J = 15/2, 17/2$ excited states. Calculated binding energies for these states are 254 meV for the $J = 8$ state relative to its $4f^{12}5d6s^2$ $J = 15/2$ threshold and 258 and 173 meV relative to the $J = 17/2$ threshold for $J = 9$ and $J = 10$, respectively. These high J $4f^{12}5d6s^26p$ states have open decay channels only to $4f^{13}6s^2$ $J = 7/2, 5/2$ and $4f^{12}5d6s^2$ $J = 9/2$, resulting in emitted electrons of symmetry ϵg , ϵh , and ϵi . The lifetimes for these long lived $J = 8, 9, 10$ states are estimated to be 9.8 μs , 0.9 ms, and 6.6 ms, respectively.

PACS numbers: 32.70.Jz, 32.70.Cs, 31.25.Jf, 31.15.Ar

I. INTRODUCTION

Recently Davis and Thompson have observed two long lived ($> 56\mu\text{s}$) states of Tm^- with electron affinities (EA) ~ 1.0 eV [1]. Existing theoretical studies, admittedly rough, of $6p$ attachment to the ground state predict an EA ~ 110 meV [2], and a $4f$ attachment was estimated to be unbound by 7.9 eV [3]. An early observation estimated the EA to be approximately 34 meV [4].

Except for the two leftmost lanthanides, La [5] and Ce [6], and the rightmost lanthanide, Lu [7], no modern result suggests ground state EA's exceeding 150 meV [4, 8–10], and bound excited states of Lanthanide anions are terra incognita. A recent extensive review of anions has been made by Andersen [11]. Thus the Davis and Thompson results [1] are so far unique. In this study, we took a more accurate look at $6p$ and $4f$ attachment to the ground state, and also provided an estimate for $5d$ attachment. We found no convincing evidence that direct attachment to the ground state of Tm I of p , d , or f electrons was possible.

We then decided to investigate the possibility that these Tm^- states [1] might correspond to attachment(s) to an excited state of the Tm I atom. A crucial property of such a candidate would be its lifetime, which would have to exceed 56 μs [1] in order to be observed. It is likely that the most rapid decay mechanism would be that of relativistic autoionization. Accurate calculation would be particularly challenging since the relativistic methodology is incomplete [12] for ions of this complexity. For example, neither a fully automated treatment of nonorthonormality (NON) nor a satisfactory treatment of open channel coupling is currently available. The candidate(s) would also have to be sufficiently well bound to an appropriate atomic threshold to yield EA's consistent with what is observed [1].

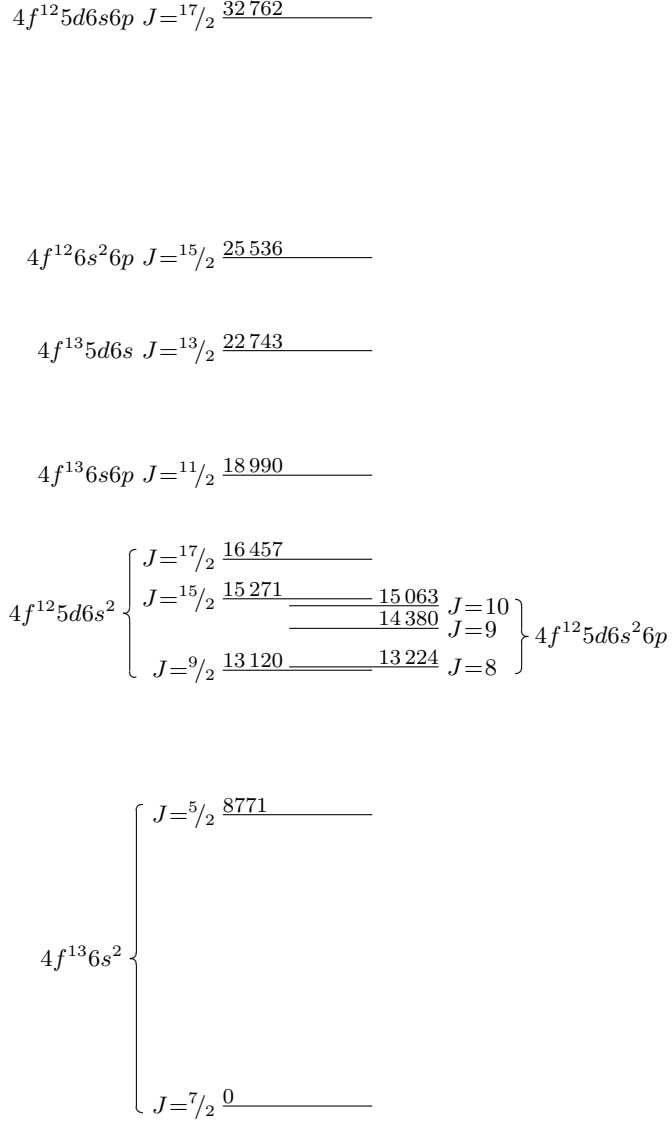
Our prime interest is in the lowest lying excited atomic configurations and their higher J states, as these should produce the fewest number of open channels and/or increase the minimum azimuthal quantum number of the ejected electron, thereby increasing the lifetime. Existing spectra [13] suggest the odd parity configurations $4f^{13}5d6s$, $4f^{12}6s^26p$, and $4f^{12}5d6s6p$ as candidates. Even parity candidates include $4f^{12}5d6s^2$ and $4f^{13}6s6p$. Possible high J thresholds [13] from these configurations are shown in Fig. 1. The odd parity atomic states lie above 20 000 cm^{-1} and the even parity ones above 13 000 cm^{-1} , so Tm^- $4f^{13}6s^2\epsilon\ell$ channels are always open. Note that the critical level in the spectrum is the $4f^{12}5d6s^2$ $J = 15/2$ level at 15 271 cm^{-1} [13]. In order to be long lived, attachments to higher levels would likely require high enough binding energies to lie below this level, otherwise the open channel to this $J = 15/2$ level would allow an ejected ϵd , ϵp , or even ϵs electron.

Our experience with negative ions suggests that attachments are more likely into already occupied subshells and also yield larger EA's, e.g. attaching a $6p$ into $6p^n$ ($n < 6$). Computationally, it is also easier to replace d or f attachment to a given level with an s or p attachment to a different level, providing both yield the same configuration. An attached electron of higher azimuthal symmetry requires a more complete treatment of the core electrons, which we would prefer to avoid. Illustrations of these points may be found elsewhere [6].

II. METHODOLOGY

For lifetime calculations, we separate the wavefunction into two orthogonal parts – the localized portion (Φ), which decays asymptotically and the open channel portion, $U_i(E)$, which is asymptotically sinusoidal. The relativistic methodology [12] is an extension of the non-relativistic methodology of Fano [14]. For $4f^{12}5d6s^26p$ states considered

FIG. 1: Potential high J Tm I thresholds. The levels on the right are the three long lived Tm⁻ states discussed in Sect. III C. Energies [13] relative to the Tm I ground state are given in cm⁻¹.



here, the open channels are formed by attaching a continuum electron to one of the three neutral atom thresholds: $4f^{13}6s^2 \ J = 7/2, 5/2$ or $4f^{12}5d6s^2 \ J = 9/2$, see Fig. 1. Orthogonality is imposed between the parts by orbital restrictions, i.e. $[4f^{13}6s^2]_{7/2,5/2} v\ell_j$ and $[4f^{12}5d6s^2]_{9/2} v\ell_j$ are excluded from the localized portion of the wavefunction.

The autoionization width for one open channel is given by:

$$\Gamma(i) = 2\pi |\langle \Phi | H_{DB} - E | U_i(E) \rangle|^2 \quad (1)$$

where the resonance energy E is found from:

$$E - E(\Phi) = \sum_i PV \int d\epsilon \frac{|\langle \Phi | H_{DB} - E | U_i(\epsilon) \rangle|^2}{(E - \epsilon)} \quad (2)$$

and the autoionization lifetime τ is given by:

$$\tau(s) = \frac{2.4189 \times 10^{-17}}{\sum_i \Gamma(i)} \quad (3)$$

In these formulae, $E(\Phi)$ is the localized energy $\langle \Phi | H_{DB} | \Phi \rangle$, where H_{DB} is the Dirac-Breit Hamiltonian, and the integral in (2) is a principal-valued one.

The methodology [12, 14] calls for the $U_i(e)$ to be orthogonal, not to interact with each other, and to be energy normalized. Within a single open channel, these conditions are satisfactorily met, by use of the frozen core approximation. The wavefunction is generated by a modified version of the continuum wavefunction solver (CONTWVSA) of Perger *et al.* [16, 17] which has recently been improved [16]. The new version is now “stand alone”, i.e. it can accept either Desclaux [15] or GRASP [18] input for the bound core radial functions, evaluate magnetic Breit radial integrals (needed for the autoionization width), and converge for high ℓ , low ϵ cases. The algorithm still lacks the ability to deal with a multi-configurational core [16]. In the case of the $[4f^{12}5d6s^2]_{9/2}\epsilon\bar{\ell}_j$ calculations we have avoided this problem (there are 12 possible eigenvectors) by using the one eigenvector dominating the Tm I threshold, $4f_{5/2}^6 4f_{7/2}^6 5d_{3/2} 6s_{1/2}^2$ (coefficient of ~ 0.888).

Our localized calculations begin with the generation of one electron wavefunctions using Desclaux’s multi-configurational Dirac-Fock (MCDF) code [15]. These DF functions are combined into determinantal many electron wavefunctions. The basis members of our relativistic configuration-interaction (RCI) calculations are linear combinations of these determinants, created as eigenstates of J^2 , J_z , and parity. Correlation consists primarily of single and double excitations with respect to the DF configuration, with some second order triple and quadruple excitations added to correlate a few important first order configurations (see Sect. III C for more details).

Excitations into subshells that are unoccupied in the DF configuration(s) include one electron “virtual” orbitals, denoted $v\ell$ ($v\bar{\ell}$) for even (odd) functions throughout this discussion. These virtual orbitals are relativistic screened hydrogenic orbitals, whose effective charges, Z^* ’s, are chosen through an energy minimization process. Such virtual orbitals represent the unoccupied Rydberg series and continuum orbitals of the same symmetry, and in this case we find two sets of virtuals sufficient to saturate the radial space, i.e. $vd + vd' \simeq 6d + 7d + 8d + \dots + \epsilon d$.

Calculations of EA’s require equal treatment of both negative ion states and the corresponding neutral threshold with regard to excitations that are present in both species as well as careful attention to exclusion effects that occur in only one of the states. For example, when treating the $6p$ attachment to a Tm I $4f^{12}5d6s^2$ state it is essential to include the same amount of correlation to $5d6s$ pair excitations both with regard to symmetry of virtuals (e.g. $5d6s \rightarrow vsvp + vpv d + vdvf + vfv g$) and saturation of virtuals (e.g. $5d6s \rightarrow vpv d + vpv d' + vp'vd + vp'vd'$). In the same example excitations into the $6p$ subshell (singly occupied in the negative ion state only), such as $6s^2 \rightarrow 6pvp$, favor the neutral threshold and tend to decrease the binding of the Tm⁻ $4f^{12}5d6s^2 6p$ state. Conversely, $(5d + 6s)6p$ pair excitations and $6p$ single excitations are present only in the negative ion state and thus serve to increase the binding energy of the system. For this study we treat the Tm⁻ $4f^{12}5d6s^2 6p$ $J = 8$ state as a $6p_{1/2}$ attachment to its natural Tm I $4f^{12}5d6s^2$ $J = 15/2$ threshold, directly comparing energies of the two states with equivalent correlation as described above. The Tm⁻ $4f^{12}5d6s^2 6p$ $J = 9, 10$ states are then positioned by comparing energies relative to the Tm⁻ $J = 8$ level. The placement of these levels (see Fig. 1) determines the energy used for the continuum function for each available channel.

An inclusive, automated code [19] that internally generates the necessary atomic structure and evaluates the matrix elements of Γ in (1) using full NON is in intermediate stages of development by our group, so several alternative auxiliary codes needed to be prepared for this project. Our approach is to break the matrix elements up by configuration, separately calculating the interaction of one (nonrelativistic) configuration in the bra and one in the ket. The data is prepared as a mock RCI calculation, e.g. for the calculation of $J = 10$ $\langle 4f^{12}5d6s^2 6p | H | 4f^{13}6s^2 \epsilon i_{13/2} \rangle$ we prepare a two configuration input file, and a modified version of the main RCI code [20] was created to suppress printing of matrix elements that do not contain one basis member from the bra ($4f^{12}5d6s^2 6p$) and one from the ket ($4f^{13}6s^2 \epsilon i$).

Changes also needed to be made in the modified version of the RCI code in the preparation of the necessary R^k integrals which arise from the expansion of the two electron Coulomb operator, $1/r_{12}$, in terms of r_1 and r_2 :

$$R^k(a, b|c, d) = \int_0^\infty \int_0^\infty [P_a^*(1)P_c(1) + Q_a^*(1)Q_c(1)] \frac{r_1^k}{r_1^{k+1}} \times [P_b^*(2)P_d(2) + Q_b^*(2)Q_d(2)] dr_1 dr_2 \quad (4)$$

These integrals are initially prepared such that the arguments a and b are subshells from the bra, and c and d are from the ket. In the case that the bra and ket differ by two electrons (a, b, c , and d all represent different nonrelativistic subshells), the application of the symmetry relation $R^k(a, b|c, d) = R^k(b, a|d, c)$ is the only simplification possible to reduce the number of stored integrals, and it does not disturb this convention. However, when the bra and ket (nonrelativistic) configurations differ by one electron other symmetry relations, such as $R^k(a, b|c, d) = R^k(c, d|a, b)$, may also reduce the number of integrals but break the convention that the first two arguments come from the bra. The modified code must then suppress the symmetry reductions, so that there is no ambiguity as to the origin of radial functions in evaluation of the matrix elements in (1). For example, in the $J = 10$ $[4f^{13}6s^2]_{7/2}\epsilon i_{13/2}$ channel, the evaluation of $\langle 4f^{12}5d6s^2 6p | H | 4f^{12}6s^2 6p \epsilon i \rangle$, would result in the unmodified code treating $R^4(4f_{5/2}, 5d_{5/2} | \widehat{4f}_{7/2}, \epsilon i_{13/2})$

and $R^k(4f_{7/2}, 5d_{5/2}|\widehat{4f}_{5/2}, \epsilon i_{13/2})$ (the “hat” indicating a radial function taken from the Tm I calculation) as equivalent, which is clearly not the case when dealing with two nonorthonormal sets of radial functions.

A second code was prepared to partially treat NON, while reading RCI coefficients from the EA calculation RCI wavefunctions. For each pair of basis members (bra and ket) the coefficient of each R^k integral is multiplied by their coefficients from the earlier RCI calculation as well as a NON coefficient containing the overlap integrals of their common subshells. For example, an integral of the form $c_0 R^k(6s_{1/2}, 6p_{3/2}|\widehat{4f}_{7/2}, \epsilon i_{13/2})$ in the matrix element between $4f_{5/2}^6 4f_{7/2}^6 5d_{5/2} 6s_{1/2}^2 6p_{3/2}$ and $\widehat{4f}_{5/2}^6 \widehat{4f}_{7/2}^7 \widehat{5d}_{5/2} \widehat{6s}_{1/2} \epsilon i_{13/2}$ would be passed to the next stage of the calculation with a new coefficient, $c_{bra} c_{ket} c_{NON} c_0$, where c_{bra} is taken from the Tm⁻ $4f^{12} 5d 6s^2 6p$ $J = 10$ calculation, c_{ket} is taken from the Tm I $4f^{13} 6s^2$ $J = 7/2$ calculation, and c_{NON} is a product of the overlap integrals of the core orbitals, $\langle 4f_{5/2} | \widehat{4f}_{5/2} \rangle^6$, $\langle 4f_{7/2} | \widehat{4f}_{7/2} \rangle^6$, $\langle 5d_{5/2} | \widehat{5d}_{5/2} \rangle$, and $\langle 6s_{1/2} | \widehat{6s}_{1/2} \rangle$. The above approach is not a full treatment of NON, as we only account for overlaps with corresponding orbitals, i.e. $\langle 6s | \widehat{6s} \rangle$ is accounted for, but $\langle vs | \widehat{6s} \rangle$ is still assumed zero, so the matrix elements $\langle 4f^{12} 5d 6s 6p vs | H | \widehat{4f}^{13} \widehat{5d} \widehat{6s} \epsilon i_{13/2} \rangle$ are effectively set to zero (the basis functions are triple excitations with respect to one another if the DF radials are treated as equivalent). Similarly, we ignore rotation of radials of the same symmetry, e.g. replacement of the above integral with one of the form $R^k(5s_{1/2}, 6p_{3/2}|\widehat{4f}_{7/2}, \epsilon i_{13/2})$ and $\langle 6s | \widehat{6s} \rangle$ with $\langle 6s | \widehat{5s} \rangle$. Since both $\langle vs | \widehat{6s} \rangle$ (~ 0.005) and $\langle 6s | \widehat{5s} \rangle$ (~ 0.020) are much smaller than $\langle 6s | \widehat{6s} \rangle$ (~ 0.995), we assume that such errors introduced by partial treatment of NON are small compared to other difficulties discussed in Sect. III C.

The R^k integrals are evaluated using a recently improved version of the continuum integral solver (CIS) code of Perger *et al.* [21, 22]. The final bit of preparation of integrals involves collecting coefficients that appear for the same R^k integral. For a typical calculation of the contribution of two configurations, there may be several hundred basis functions in either the bra or the ket. Though not every pair of basis functions within those two nonrelativistic configurations produce R^k integrals, those that do often duplicate integrals that appear in other pairs. To speed up the process of our final evaluations we first sum over the coefficients produced as described above so that for a given pair of bra/ket configurations, each R^k integral is only evaluated once. The savings can be a factor of 20 or greater, and many of the evaluations over these pairs of configurations could take two hours or more on our 500 MHz Alpha Workstation without it.

III. RESULTS

A. Ground State Attachments

Chevary and Vosko’s [2] estimated EA for the $4f^{13} 6s^2 6p$ $J = 3$ state is 110 meV with an estimated uncertainty of 54 meV, using Dirac-Hartree-Fock (DHF) density functional theory. They were unable to obtain a DHF solution for Tm⁻, instead extrapolating this portion of the EA from the closest Z (69.1) for which they were able to obtain a solution. Correlation effects were treated using density functional theory.

We have managed to generate a DHF solution for Tm⁻ ($Z = 69.0$) by using a multi-configurational approach for $4f^{13}(6s + 5d)^2 6p + 4f^{13} 6p^3$. Inclusion of the $6s \rightarrow 5d$ excitation is particularly important in generating a converged solution for many anion states. We then proceeded to include single and double valence excitations into s , p , d , and f virtuals. Each virtual was represented by a single RSH, except for the p symmetry which had three virtuals. For the atomic threshold state we only included $4f^{13}(6s + 5d)^2$ and $4f^{13} 6p^2$ configurations. At this stage, the Tm⁻ is unbound by 48 meV. Since the anion is over-correlated, at least at the valence stage, compared to the atom, we inferred that it was not likely that the anion would be substantially bound if a more thorough treatment were done, so calculation efforts ceased. The results should be regarded as inconclusive regarding whether a shape resonance exists.

Our 1993 RCI study of a possible $4f$ attachment to the Tm I ground state predicted this level to be unbound by 7.9 eV [3]. This study only included the differential contributions to the EA from pair excitations from the $4f$ subshell. Virtual symmetries from $\ell = 0$ to 6 were included with vd^2 , vf^2 , and vg^2 the main contributors to the EA.

In this work, we include the “cross pairs” ($4f, 3d + 4s + 4p + 4d + 5s + 5p + 6s$) which contribute to the EA an estimated 111, 45, 168, 693, 139, 582, 11 meV, respectively. This means we now predict the $4f$ attachment to be unbound by ~ 6.2 eV. Our estimate is obtained by computing these pair effects for Tm⁻ and scaling them by 1/14 to approximate their effect on the EA [3, 23]. Use of this scale factor presumes there is little change in the radials in going from the anion to atom. Since we have ignored the effects of single symmetry changing excitations and exclusion effects ($nln'l' \rightarrow 4fv'l''$) in the atom, which will only increase the unboundedness, we see no evidence that a $4f$ attachment is bound. A possible $5d$ attachment to the atomic ground state is discussed in Sect. III B.

B. Excited State Survey

So far, only He^- , Be^- , Ar^- , and Ba^- have been found to have long lived ($>0.26 \mu\text{s}$) excited states [24]. Of these, Ba^- is potentially the most interesting in the present instance, as the state is $5d6s6p$ (^4F) $J = 9/2$. The decay is only into the ground state $6s^2\epsilon h$ continuum by means of the Breit operator. The decay time has been estimated to be in the range 1–5 ms [24, 25]. If the $4f^n$ electrons in the transition metal atom were to be essentially inactive, and the valence electrons were coupled as in Ba^- , one might hope to produce a long lived excited state. On the other hand, a $J = 9/2$ valence electron coupling requires that both the $5d$ and $6p$ electrons have their maximum j 's ($5/2$ and $3/2$, respectively) and these two are likely less bound than their “partners” $5d_{3/2}$ and $6p_{1/2}$. DHF calculation on the $4f^{13}5d6s6p$ ^5I $J = 8$ state using Desclaux's program [15] fails to converge, i.e. the $5d_{5/2}$ eigenvalue approaches zero for $Z < 69.05$. Anion states normally converge, when they do, by using somewhat higher Z converged radial functions as input. Approaching the anion Z , changes in Z in the range 0.02–0.05 are typical for convergence of consecutive solutions.

Continuing with the odd parity atomic thresholds, a $6s$ attachment to $4f^{13}5d6s$ calculated as $4f^{13}(5d_{3/2} + 6s)^3$ fails to converge for $J = 2$ or $J = 5$ for $Z < 69.4$. This also suggests that a $5d$ attachment to the ground state is unbound. The same inference can be drawn (for $5d$ and $6p$ attachment to the ground state) since s attachments to ground state configurations have EA's in the range of 0.5–1.3 eV [24], with the higher end associated with transition metal atoms. For the $5d$ and $6p$ ground state Tm I possible attachments, the relevant excited state Tm I thresholds (for s attachment) lie > 2.0 eV above the Tm I ground state, which considerably exceeds the known $6s$ attachment range [24].

C. Three Long Lived Excited States

As presented in Fig. 1 we find from our EA calculations three candidates for long lived attachments to high J Tm I excited thresholds. These are $6p$ attachments to the two closely spaced $J = 15/2$ and $J = 17/2$ $4f^{12}5d6s^2$ thresholds. The $4f^{12}5d6s^2$ $J = 8$ and $J = 10$ states are clearly a $6p_{1/2}$ attachment to $J = 15/2$ and a $6p_{3/2}$ attachment to $J = 17/2$, respectively. Analysis of coefficients of basis members in the $J = 9$ calculation indicate that it is predominantly a $6p_{1/2}$ attachment to $4f^{12}5d6s^2$ $J = 17/2$, but there is approximately 35% mixing with basis members representing a $6p_{3/2}$ attachment to $J = 15/2$. As mentioned in Sect. I, all three lie below the $J = 15/2$ threshold ($J = 8$ bound by 254 meV to the $J = 15/2$ threshold and $J = 9, 10$ bound to the $J = 17/2$ threshold by 258 and 173 meV, respectively), which allows only high azimuthal quantum number ejected electrons in the $[4f^{13}6s^2]_{7/2,5/2}\epsilon\ell_j$ and $[4f^{12}5d6s^2]_{9/2}\epsilon\ell_j$ channels.

As mentioned in Sect. II correlation in the ket is determined from the Tm I calculation. For example, in calculating the $J=10$ matrix element $\langle 4f^{12}5d^26s6p|H|4f^{13}5d6s\epsilon i\rangle$, the basis members of the ket are created by restricting the continuum function to $\epsilon i_{13/2}$ and the J of the $4f^{13}5d6s$ subgroup to $7/2$. Careful treatment of the data preparation ensures that each basis member of $[4f^{13}5d6s]_{7/2}\epsilon i$ has a one to one correspondence (properly ordered) with each basis member of the $4f^{13}5d6s$ configuration in the $J = 7/2$ calculation, which supplies the RCI coefficients.

RCI correlation includes all single and double excitations out of the $5d6s^26p$ (Tm $^-$), $5d6s^2$ (Tm I $J = 9/2$), and $6s^2$ (Tm I $J = 7/2, 5/2$) subgroups as well as $4f6s$ pair excitations in the $4f^{13}6s^2$ calculations (configurations with $4f^{13}$ and $4f^{11}$ subgroups in the $4f^{12}5d6s^26p$ and $4f^{12}5d6s^2$ calculations were found to have negligible correlation effects). Additional second order effects were included in the form of added correlation to the important configurations resulting from $6s \rightarrow 5d$ and $6s^2 \rightarrow 6p^2$ (typical mixing of 1.0% to 3.5%) in each species, e.g. the $4f^{12}5d6s^26p$ calculations include configurations of the form $4f^{12}5d^2v\bar{v}\bar{v}$, $4f^{12}5d^3v\bar{v}$, $4f^{12}6p^2v\bar{v}\bar{v}$, and $4f^{12}6p^3v\bar{v}$.

Contributions to the autoionization width of each important decay channel are presented in Tables I and II. The dominant decay channel for each $4f^{12}5d6s^26p$ Tm $^-$ state is to $[4f^{13}6s^2]_{7/2}\epsilon\ell_{\ell+1/2}$ (with minimum ℓ to make the total $J = 8, 9, 10$). For $J = 8, 10$ this is the only channel with a continuum function of this symmetry. For $J = 9$ two other channels with the same ℓ are available, $[4f^{13}6s^2]_{5/2}\epsilon i_{13/2}$ and $[4f^{13}6s^2]_{7/2}\epsilon i_{11/2}$. The former is several orders of magnitude slower (see effective lifetime in Table I) than the dominant channel, while the latter is of the same order. For $J = 8, 10$ the corresponding channels require $\ell' = \ell + 2$, i.e. $[4f^{13}6s^2]_{5/2}\epsilon\ell'_{\ell'+1/2}$ and $[4f^{13}6s^2]_{7/2}\epsilon\ell'_{\ell'+1/2}$. Intermediate calculations (not shown in Table I) suggest these channels of higher symmetry are 5–6 orders of magnitude slower than the dominant $[4f^{13}6s^2]_{7/2}\epsilon\ell_{\ell+1/2}$ channel. As shown in Table II, $[4f^{12}5d6s^2]_{9/2}\epsilon\bar{\ell}_{\bar{\ell}+1/2}$ ($\bar{\ell} = \ell - 1$) channels are approximately 50–100 times slower than the corresponding $[4f^{13}6s^2]_{7/2}\epsilon\ell_{\ell+1/2}$ channels. As in the decay to the Tm I odd levels, an additional channel is available for $J = 9$, i.e. $[4f^{12}5d6s^2]_{9/2}\epsilon\bar{\ell}_{\bar{\ell}-1/2}$ ($\epsilon h_{9/2}$), which is ~ 10 times slower than the dominant (ground state) channel. The channels presented in Table II are slower than the $[4f^{13}6s^2]_{7/2}\epsilon\ell_{\ell+1/2}$ ground state channels with higher ℓ due to the much smaller value of ϵ in the continuum function (see energy differences in Fig. 1). For comparison, an auxiliary calculation was made for $J = 10$ for which the $\epsilon h_{11/2}$ energy was adjusted to

TABLE I: $\text{Tm}^- 4f^{12}5d6s^26p$ $J = 8, 9, 10$ contributions to $4f^{13}6s^2\epsilon\ell$ autoionization widths. Entries marked $\langle\text{DF}|\text{DF}\rangle$ include $4f^{12}(5d+6s)^36p$ and $4f^{12}(5d+6s)6p^3$; $|\text{DF}\rangle$ includes $4f^{13}(5d+6s)^2\epsilon\ell$, $4f^{13}6p^2\epsilon\ell$, $4f^{12}(5d+6s)^26p\epsilon\ell$, and $4f^{12}6p^3\epsilon\ell$; and $\langle 2\text{O}|\text{DF}\rangle$ ($|\text{2O}\rangle$) includes second order configurations, triple and quadruple excitations with respect to $4f^{12}5d6s^26p$ ($4f^{13}6s^2\epsilon\ell$). Energies are presented in units of 10^{-9} a.u.

Contribution	$J = 8$	$J = 9$	$J = 9$	$J = 9$	$J = 10$
	$[4f^{13}6s^2]_{7/2}\epsilon g_{9/2}$	$[4f^{13}6s^2]_{7/2}\epsilon i_{11/2}$	$[4f^{13}6s^2]_{7/2}\epsilon i_{13/2}$	$[4f^{13}6s^2]_{5/2}\epsilon i_{13/2}$	$[4f^{13}6s^2]_{7/2}\epsilon i_{13/2}$
$\langle\text{DF} \text{DF}\rangle$	4435.83	5.47	-27.23	0.18	-37.50
$\langle\text{DF} \text{H} 4f^{12}6s^2v\bar{\ell}\epsilon\ell\rangle$	785.48	0.55	3.52	0.17	0.90
$\langle\text{DF} \text{H} 4f^{12}6s6pv\bar{\ell}\epsilon\ell\rangle$	-2455.59	3.36	36.54	0.17	-7.82
$\langle\text{DF} \text{H} 4f^{12}5d6sv\bar{\ell}\epsilon\ell\rangle$	-232.23	0.06	-0.17	0.00	0.09
$\langle\text{DF} \text{H} \text{2O}\rangle$	-82.92	-1.24	3.44	-0.08	-0.75
$\langle 4f^{12}5d6s^2v\bar{\ell} \text{H} \text{DF}+\text{X}^a\rangle$	-1122.59	-9.81	-48.13	-0.74	-5.81
$\langle 4f^{12}5d6s6pv\bar{\ell} \text{H} \text{DF}+\text{X}^a\rangle$	251.72	3.99	-41.17	-0.02	-2.28
$\langle 4f^{12}6s^26pv\bar{\ell} \text{H} \text{DF}+\text{X}^a\rangle$	-2164.30	-5.63	8.09	0.27	-7.44
$\langle 4f^{12}5d^26sv\bar{\ell} \text{H} \text{DF}+\text{X}^a\rangle$	39.03	1.11	10.76	0.03	1.85
$\langle 4f^{12}5d6sv\bar{\ell} \text{H} \text{DF}+\text{X}^a\rangle$	-62.39	-0.38	-4.05	-0.01	-1.05
$\langle 4f^{12}5d6p^2v\bar{\ell} \text{H} \text{DF}+\text{X}^a\rangle$	-209.50	-0.82	-3.36	-0.10	-0.54
$\langle 4f^{12}5d^26pv\bar{\ell} \text{H} \text{DF}+\text{X}^a\rangle$	-102.25	-2.42	-1.59	-0.01	-2.65
$\langle 4f^{12}5d6pv\bar{\ell}^2 \text{H} \text{DF}+\text{X}^a\rangle$	9.18	0.48	-0.33	-0.02	0.19
$\langle 4f^{12}6s^2v\bar{\ell} \text{H} \text{DF}+\text{X}^a\rangle$	1835.64	22.19	78.17	1.18	18.65
$\langle 4f^{12}6s6p^2v\bar{\ell} \text{H} \text{DF}+\text{X}^a\rangle$	-491.92	3.33	23.23	0.05	11.38
$\langle 4f^{12}6s6pv\bar{\ell}^2 \text{H} \text{DF}+\text{X}^a\rangle$	-7.66	2.91	15.35	0.05	0.97
$\langle 2\text{O} \text{H} \text{DF}+\text{X}^a\rangle$	201.46	0.76	2.76	0.05	7.83
Total	626.99	23.91	55.83	1.17	-23.98
Effective Lifetime	9.8 μs	6.7 ms	1.2 ms	2.8 s	6.7 ms

^aThe $J = 8$ calculation also includes all correlation in the ket.

^bEntries with $v\bar{\ell}^2$ include $v\bar{\ell}^2$, $vlv\bar{\ell}$, and $v\bar{\ell}v\bar{\ell}$.

match the $\epsilon i_{13/2}$ function in the calculation of the ground state channel. The effective lifetime of this (nonphysical) calculation is approximately three orders of magnitude smaller than the calculation with the correct energy.

As an illustration of the effects of NON in these calculations, we performed several auxiliary calculations that neglect the partial NON treatment as discussed in Sect II. Typical values for the overlap integrals are >0.99 for the core, $4f$, and $6s$ subshells, $0.90-0.99$ for $5d$, and $0.85-0.95$ for the $6p$ subshell; i.e. c_{NON} varies from ~ 0.80 to ~ 0.97 , depending on which subshells the bra and ket have in common. Cancellation of contributions decreases this effect, i.e. the autoionization width is not simply reduced by c_{NON} , but the effect is not negligible. For example, the $\langle\text{DF}|\text{H}|\text{DF}\rangle$ contribution of the $[4f^{13}6s^2]_{7/2}\epsilon g_{9/2}$ $J = 8$ autoionization width is $\sim 6.9\%$ larger with the omission of the partial NON treatment, suggesting that this correction affects the effective lifetime of a given channel by $10-15\%$.

For purposes of analysis, we break down contributions to autoionization widths in terms of bra and ket configurations. The largest (in terms of RCI coefficients) configurations for each calculation involve those configurations that represent excitation into the DF radial functions, i.e. those that do not contain virtual functions. These are collected as “DF” in Tables I and II, and other configurations are collected by type. We include in our calculations all matrix elements with these DF configurations in the either the bra or ket (or both), except where described below. This approach assumes that matrix elements with small coefficient configurations in both the bra and ket will be small with respect to the above contributions (the proposed automated code would not make such an approximation).

While the amount of cancellation from the DF to the total correlated autoionization width is large (nearly an order of magnitude in the $[4f^{13}6s^2]_{7/2}\epsilon g_{9/2}$ $J = 8$ case) much of it is due to saturation of the basis set. Configurations representing single excitations from the DF configuration can be considered as providing corrections to the DF one electron radial functions. For example, in the $[4f^{13}6s^2]_{7/2}\epsilon g_{9/2}$ $J = 8$ calculation we could collect the contributions with regard to “pseudo-configurations” with the bra configurations $4f^{12}5d6s^26p$, $4f^{12}vd6s^26p$, and $4f^{12}5d6s^2vp$ grouped together, greatly reducing the apparent cancellation of some of the largest contributions in Table I (the 4435.83, -1122.59 , and -2164.30 entries are dominated by these configurations, and such a reorganization would effectively add these together to one contribution of ~ 1150). Even so, we note that there is still a great deal of contribution to this $J = 8$ calculation from configurations which are relatively small in other channels. In this case we expand our calculation to include configurations with virtual orbitals (labeled X in Table I) in both the bra and ket, thus including the sum over all matrix elements (using the same notation the other channels exclude $\langle X|\text{H}|X\rangle$ contributions). The

TABLE II: Tm⁻ $4f^{12}5d6s^26p$ $J = 9, 10$ contributions to $4f^{12}5d6s^2\bar{\epsilon}\bar{\ell}$ autoionization widths. Entries marked ⟨DF| include $4f^{12}(5d+6s)^36p$ and $4f^{12}(5d+6s)6p^3$; |DF⟩ includes $4f^{12}(5d+6s)^3\bar{\epsilon}\bar{\ell}$ and $4f^{12}(5d+6s)6p^2\bar{\epsilon}\bar{\ell}$; and ⟨2O| (|2O⟩) includes second order configurations, triple and quadruple excitations with respect to $4f^{12}5d6s^26p$ ($4f^{12}5d6s^2\bar{\epsilon}\bar{\ell}$). Energies are presented in units of 10^{-9} a.u.

Contribution	$J = 9$	$J = 9$	$J = 10$
	$[4f^{12}5d6s^2]_{9/2}\epsilon h_{9/2}$	$[4f^{12}5d6s^2]_{9/2}\epsilon h_{11/2}$	$[4f^{12}5d6s^2]_{9/2}\epsilon h_{11/2}$
⟨DF H DF⟩	-21.66	-0.90	72.40
⟨DF H $4f^{12}5d6s^2v\bar{\ell}\bar{\epsilon}\bar{\ell}$ ⟩	1.80	-0.46	-4.72
⟨DF H $4f^{12}6s^2v\bar{\ell}\bar{\epsilon}\bar{\ell}$ ⟩	-2.09	0.21	0.60
⟨DF H $4f^{12}5d6pv\bar{\ell}\bar{\epsilon}\bar{\ell}$ ⟩	0.09	-0.08	-0.42
⟨DF H $4f^{12}5d^2v\bar{\ell}\bar{\epsilon}\bar{\ell}$ ⟩	-0.09	-0.01	-0.23
⟨DF H $4f^{12}6s6pv\bar{\ell}\bar{\epsilon}\bar{\ell}$ ⟩	4.42	-3.56	-22.81
⟨DF H 2O⟩	-0.39	-0.07	10.78
⟨ $4f^{12}5d6s^2v\bar{\ell}$ H DF⟩	1.88	2.02	62.87
⟨ $4f^{12}5d6s6pv\bar{\ell}$ H DF⟩	-3.89	-0.51	-16.58
⟨ $4f^{12}6s^26pv\bar{\ell}$ H DF⟩	20.53	-2.84	29.78
⟨ $4f^{12}5d^26sv\bar{\ell}$ H DF⟩	1.16	0.63	6.85
⟨ $4f^{12}5d6sv\bar{\ell}$ H DF⟩	0.62	-0.16	-1.78
⟨ $4f^{12}5d6p^2v\bar{\ell}$ H DF⟩	0.54	-0.18	3.34
⟨ $4f^{12}5d^26pv\bar{\ell}$ H DF⟩	-0.24	0.14	-1.31
⟨ $4f^{12}5d6pv\bar{\ell}^2$ H DF⟩	0.07	0.01	-0.59
⟨ $4f^{12}6s^2v\bar{\ell}$ H DF⟩	-19.19	-2.33	-139.56
⟨ $4f^{12}6s6p^2v\bar{\ell}$ H DF⟩	1.22	-0.17	4.98
⟨ $4f^{12}6s6pv\bar{\ell}^2$ H DF⟩	-0.16	-0.15	0.84
⟨2O H DF⟩	-0.84	-0.05	-6.59
Total	-16.22	-8.46	-2.15
Effective Lifetime	14.6 ms	53.7 ms	0.8 s

^aEntries with $v\bar{\ell}^2$ include $v\bar{\ell}^2$, $vlv\bar{\ell}$, and $v\bar{\ell}v\bar{\ell}$.

final autoionization width presented in Table I for this channel is approximately twice the incomplete sum (i.e. the lifetime is decreased by a factor of ~ 4).

Combining the effective lifetimes for the channels presented in Tables I and II results in estimated lifetimes for the Tm I $4f^{12}5d6s^26p$ $J = 8, 9, 10$ of 9.8 μ s, 0.9 ms, and 6.6 ms, respectively. As mentioned in Sect. II, our current methodology does not support mixing between configurations with differing continuum functions, nor does our main RCI code [20] allow calculations with continuum functions. We can, however, approximate the effects of a continuum functions using a diffuse (small Z^*) virtual orbital. A separate RCI calculation for the $J = 9$ ϵi was made using a vi replacement virtual with $Z^* \sim 0.5$. Relaxation of the core J in this calculation allows simultaneous calculation of the $[4f^{12}5d6s^26p]_{7/2}vi_{13/2}$, $[4f^{12}5d6s^26p]_{7/2}vi_{11/2}$, and $[4f^{12}5d6s^26p]_{5/2}vi_{13/2}$ states. However, the localized and “pseudo-continuum” portions of these wavefunctions are sufficiently isolated that there is minimal mixing ($< 1\%$) between these states. In fact, the calculation essentially reproduces the Tm I spectrum with two nearly degenerate states from the above basis functions with the $J = 7/2$ core and one from the basis function with the $J = 5/2$ core at approximately the same energy difference as the $J = 5/2$ $4f^{13}6s^2$ level (see Fig. 1). Due to this lack of mixing we have treated each of the previously mentioned $J = 9$ cases with two continua of equal energy as separate channels for purposes of lifetime calculation.

Accuracy of these lifetimes is reduced for several reasons. The $\langle X|H|X \rangle$ contributions absent from the $J = 9$ and $J = 10$ calculations would likely affect the total less than in the $J = 8$ case, but may not be insignificant. Also, the second order effects introduced to correlate important configurations in the EA calculation are themselves large contributors to the autoionization widths. This suggests there may be other triple and quadruple excitations that are missing that may also be nonnegligible, e.g. $4f^{12}5d^2v\bar{\ell}\bar{\epsilon}\bar{\ell}$ is not present in the ket for the $[4f^{13}6s^2]_{7/2}\epsilon i_j$ channels but could have a large matrix element with $4f^{12}5d^2v\bar{\ell}\bar{\epsilon}\bar{\ell}$ in the bra. For $J = 8$ we have presented the $[4f^{13}6s^2]_{7/2}\epsilon g_{9/2}$ channel only. As previously mentioned, intermediate calculations indicate the $[4f^{13}6s^2]_{5/2}\epsilon i_{11/2}$ channel is negligible to the lifetime. Test calculations for the $[4f^{12}5d6s^2]_{9/2}\epsilon f_{7/2}$ channel give an effective lifetime approximately an order of magnitude larger than the $[4f^{13}6s^2]_{7/2}\epsilon g_{9/2}$ value presented in Table I, suggesting this channel may have some impact on the $J = 8$ lifetime. However, our typical EA calculations are accurate to 2–300

cm^{-1} , and are likely to err toward a binding energy that is too small. Thus, the position of the $\text{Tm}^- J = 8$ level $\sim 100 \text{ cm}^{-1}$ above the $\text{Tm I } J = 9/2$ threshold is not sufficient to indicate whether this channel is even open, which is why we have omitted a more thorough treatment of this calculation. Considering the potential error in placement of the Tm^- levels, auxiliary calculations were made by altering several continuum function energies by 250 cm^{-1} , and the resulting changes to autoionization width contributions were approximately 3–4%. Finally, there are changes between intermediate and final calculations that suggest changes in autoionization widths of a factor of two simply due to changes in the wavefunctions from saturation of the virtual basis, addition of second order effects, and inclusion of the Breit operator in the RCI calculations. This last step, inclusion of the Breit operator, affects the autoionization widths by approximately 5%, but explicit calculation of radial integrals involving the Breit operator in (1) were found to be negligible, 3–4 orders of magnitude smaller than the corresponding R^k integrals.

IV. CONCLUSION

RCI calculations predict three long lived $4f^{12}5d6s^26p$ states of Tm^- bound to two $\text{Tm I } 4f^{12}5d6s^2$ thresholds: $J = 8$ ($9.8 \mu\text{s}$) bound to $\text{Tm I } J = 15/2$ by 254 meV, $J = 9$ (0.9 ms) bound to $\text{Tm I } J = 17/2$ by 258 meV, and $J = 10$ (6.6 ms) bound to $\text{Tm I } J = 17/2$ by 173 meV. The latter two lifetimes are well above the $56 \mu\text{s}$ limit of the apparatus of the recent experiment [1], and have a similar splitting (85 meV vs the experimental value of 50 meV [1]). Neither these binding energies nor possible weakly bound attachments to the Tm I ground state [2] (see Sect. III A) agrees with the experimental EA's of 1.029 and 0.979 eV.

However, there may be a possibility that the experiment is leaving the Tm atom in a more highly excited state, which then would produce much higher EA's. Consideration of the Tm I spectrum suggests two possibilities: excited states of $4f^{12}5d6s^2$ lying at or above 22791 cm^{-1} [13] (“EA” $\sim 1.03 \text{ eV}$), which would be created by a $6p$ detachment, or $4f^{12}6s^26p$ states, e.g. $J = 13/2$ at 22902 cm^{-1} [13] (“EA” $\sim 1.06 \text{ eV}$), if the detachment was from $5d$. Calculated photoionization cross-sections, not yet available should be quite helpful in eliminating or (possibly) confirming these options.

Acknowledgments

This work is supported by National Science Foundation grant no: PHY-0097111.

-
- [1] V. T. Davis and J. S. Thompson, Phys. Rev. A **65**, 010501 (2001).
 - [2] J. A. Chevary and S. H. Vosko, J. Phys. B **27**, 657 (1994).
 - [3] D. Datta and D. R. Beck, Phys. Rev. A **47**, 5198 (1993).
 - [4] M.-J. Nadeau, M. A. Garwan, X. L. Zhao, and A. E. W. Litherland, Nuc. Inst. Meth. B **123**, 521 (1997).
 - [5] S. M. O'Malley and D. R. Beck, Phys. Rev. A **60**, 2558 (1999).
 - [6] S. M. O'Malley and D. R. Beck, Phys. Rev. A **61**, 034501 (2000).
 - [7] S. M. O'Malley and D. R. Beck, J. Phys. B **33**, 4337 (2000).
 - [8] K. Dinov and D. R. Beck, Phys. Rev. A **51**, 1680 (1995).
 - [9] E. N. Avgoustoglou and D. R. Beck, Phys. Rev. A **55**, 4143 (1997).
 - [10] H. H. Andersen, T. Andersen, and U. V. Pedersen, J. Phys. B **31**, 2239 (1998).
 - [11] T. Andersen, Phys. Rept. **394**, 157 (2004).
 - [12] Z. Cai, D. R. Beck, and W. F. Perger, Phys. Rev. A **53**, 4660 (1991).
 - [13] W. C. Martin, B. Zalubas, and L. Hagan, Atomic Energy Levels - the Rare Earth Elements, NSRDS-NBS60 (U.S. GPO, Washington, DC, 1978).
 - [14] U. Fano, Phys. Rev. **124**, 1866 (1961).
 - [15] J. P. Desclaux, Comp. Phys. Commun. **9**, 31 (1975).
 - [16] M. G. Tews and W. F. Perger, Comp. Phys. Commun. **141**, 205 (2001).
 - [17] W. F. Perger, Z. Halabuka, D. Trautmann, Comp. Phys. Commun. **76**, 250 (1993).
 - [18] F. A. Parpia, C. Froese Fischer, and I. P. Grant, Comput. Phys. Commun. **94**, 249 (1996).
 - [19] D. R. Beck, RAUTO code, unpublished.
 - [20] D. R. Beck, RCI code, unpublished.
 - [21] W. F. Perger and V. Karighattan, Comp. Phys. Commun. **66**, 392 (1991).
 - [22] M. G. Tews and W. F. Perger, private communication.
 - [23] D. R. Beck and C. A. Nicolaidis in Excited States in Quantum Chemistry, edited by C. A. Nicolaidis and D. R. Beck, D. Reidel, Dordrecht, 1978, p. 105ff.

- [24] T. Andersen, H. K. Haugen, and H. Hotop, *J. Phys. Chem. Ref. Data* **28**, 1511 (1999).
- [25] P. L. Norquist, M. Tews, D. R. Beck, *Bull. Am. Phys. Soc.* **46**, 31 (2001).